Perspective: Current advances in solid-state NMR spectroscopy

Sharon E. Ashbrook, and Paul Hodgkinson

Citation: The Journal of Chemical Physics **149**, 040901 (2018); doi: 10.1063/1.5038547
View online: https://doi.org/10.1063/1.5038547
View Table of Contents: http://aip.scitation.org/toc/jcp/149/4
Published by the American Institute of Physics

Perspective: Current advances in solid-state NMR spectroscopy

Sharon E. Ashbrook[1,a)] and Paul Hodgkinson[2,a)]
[1]*School of Chemistry, EaStCHEM and Centre of Magnetic Resonance, University of St Andrews, St Andrews KY16 9ST, United Kingdom*
[2]*Department of Chemistry, Durham University, Durham DH1 4RD, United Kingdom*

(Received 3 May 2018; accepted 24 June 2018; published online 23 July 2018)

In contrast to the rapid and revolutionary impact of solution-state Nuclear Magnetic Resonance (NMR) on modern chemistry, the field of solid-state NMR has matured more slowly. This reflects the major technical challenges of much reduced spectral resolution and sensitivity in solid-state as compared to solution-state spectra, as well as the relative complexity of the solid state. In this perspective, we outline the technique developments that have pushed resolution to intrinsic limits and the approaches, including ongoing major developments in the field of Dynamic Nuclear Polarisation, that have enhanced spectral sensitivity. The information on local structure and dynamics that can be obtained using these gains in sensitivity and resolution is illustrated with a diverse range of examples from large biomolecules to energy materials and pharmaceuticals and from both ordered and highly disordered materials. We discuss how parallel developments in quantum chemical calculation, particularly density functional theory, have enabled experimental data to be translated directly into information on local structure and dynamics, giving rise to the developing field of "NMR crystallography." *Published by AIP Publishing.* https://doi.org/10.1063/1.5038547

I. INTRODUCTION

Nuclear Magnetic Resonance (NMR) spectroscopy has a long history of application for structure determination in systems ranging from small molecules to large proteins in solution-based experiments. The interactions experienced by the nuclear spins provide a unique sensitivity to the local structure, enabling species with different chemical environments to be resolved in the NMR spectrum. By contrast, the use of solid-state NMR spectroscopy has been limited by the anisotropic nature of NMR interactions, which broadens the spectral lines in the absence of molecular motion. This leads to loss of the vital site-specific information, reducing the structural insight that can be readily obtained. On the other hand, the measurement of these anisotropic components of the interactions can potentially provide an even greater amount of structural information in the solid state.

Spectroscopic approaches do not rely on the presence of periodic order, and so are of particular interest for characterising solids exhibiting some form of disorder (be it a variation in the nature of an atom occupying a particular site, or a variation in the positions of atoms or groups). They are, therefore, directly complementary to methods based on Bragg diffraction, where the structural models are effectively averages over space and time. Moreover NMR is also able to probe dynamics on time scales that range from ps to hundreds of seconds, allowing static and dynamic disorder to be distinguished and the nature and rate of motional processes in solids to be characterised in detail.

To realise the potential of solid-state NMR spectroscopy, it is necessary to address several challenges, not least of which is the need to improve resolution—to remove the effects of anisotropy and to enable site-specific information to be determined. An additional and enduring theme has been the need to improve sensitivity, both to overcome the inherently low Boltzmann population difference of NMR transitions and to facilitate increasingly complex experiments involving the transfer of magnetisation between nuclear spins (e.g., to probe covalent connectivity and through-space proximity of chemical species). A final challenge lies in understanding and interpreting the spectra obtained; assigning the resonances observed to specific types of chemical environments and extracting detailed structural information, both qualitative and quantitative. In this perspective, we describe the current state-of-the-art in this field, the recent advances both in hardware and methodology, and the applications they have enabled. We discuss approaches for obtaining high-resolution spectra, methods by which sensitivity can be improved, and how experimental spectroscopy can be combined with theoretical calculations to understand the local structure and disorder in a range of solids. The diversity of the field means that a full review is unfeasible; where possible, readers are referred to review articles on individual topics. Many of the examples are illustrated from our own work. A more comprehensive coverage of the primary literature can be found in the original references.

II. THE CHALLENGE OF RESOLUTION

All NMR interactions, such as the couplings between pairs of spins, are described by rank 2 tensors.[1–3] At high magnetic fields (the typical conditions for high-resolution NMR), the

a)Authors to whom correspondence should be addressed: sema@st-andrews.ac.uk and paul.hodgkinson@durham.ac.uk

Zeeman interaction between the spins and the magnetic field dominates, and the system can be conveniently described using a rotating frame in which (to first order) the "spin Hamiltonian" retains only terms that commute with the Zeeman interaction. As discussed below, this first-order approximation breaks down for quadrupolar nuclei, i.e., those with spin quantum number $I > 1/2$. This spin Hamiltonian is intrinsically orientation dependent, i.e., depends on the orientation of the NMR interaction tensors with respect to the applied field. As a result, the NMR spectrum from a sample of a powdered solid is the superposition of the spectra associated with different particle orientations. Such "wideline" NMR spectra are useful in some specialised applications, but the resulting broad "powder patterns" obscure chemical site resolution. (In the solution state, rapid molecular tumbling reduces the NMR interaction tensors to their orientation-independent isotropic average.) The rank 2 tensor nature of the NMR interactions means, however, that they have a common orientation dependence, proportional to $(3\cos^2\theta - 1)/2$, where θ is the angle between the principal axis of the tensor and the external magnetic field. As a result, if the sample is rotated about an axis oriented at the so-called "magic angle," $\theta_m = \cos^{-1}(1/\sqrt{3}) = 54.74°$, the anisotropic components of the tensor are averaged to zero, in the limit that the spinning rate is sufficiently high. Such "magic-angle spinning" (MAS), pioneered independently by Andrew and Lowe in the late 1950s, is the cornerstone of high-resolution solid-state NMR.

MAS is not, however, a panacea for problems of resolution, even for non-quadrupolar (i.e., spin $I = 1/2$) nuclei. In particular, "sufficiently high" spinning rates are difficult to achieve in ^{1}H NMR. The high magnetic dipole moment of the ^{1}H nucleus, the ubiquity of hydrogen in typical organic compounds, and the particular form of the spin Hamiltonian for coupled like spins (homonuclear coupling) mean that ^{1}H linewidths are broad and only reduce relatively slowly (linearly under most circumstances[4]) as the spinning rate increases. Historically, the limitations of simple MAS for ^{1}H (and to a lesser extent ^{19}F) NMR have been addressed using specialised radio-frequency (RF) pulse trains to manipulate the ^{1}H magnetisation in order to average out the effect of the dipolar couplings.[5,6] While such "homonuclear decoupling" has important applications, it also has significant technical challenges. Recent years have seen significant progress in improving ^{1}H resolution using ultra-fast MAS. This has involved the development of ever-smaller MAS rotors, capable of spinning rates above 100 kHz. Fortunately the efficiency of coupling between the RF and the sample increases as the RF coil size reduces, and the reduced sensitivity due to the decreased sample volume is not significant for a receptive nucleus like ^{1}H. Indeed, the tiny sample volumes are a major attraction for biomolecular NMR studies. Coupled with advances in sample preparation, such as partial deuteration to reduce the density of the coupled ^{1}H network, these developments have resulted in spectacular improvements in resolution, to the point where the solid-state biomolecular NMR spectra begin to resemble those from solution-state NMR, as illustrated in Fig. 1. Although a very dynamic field in its own right,[7,8] this perspective generally focusses on applications of solid-state NMR spectroscopy in the physical sciences.

For other spin $I = 1/2$ nuclei, such as ^{13}C, MAS is an effective means to average out anisotropic interactions, such as the chemical shift anisotropy (CSA), that would otherwise reduce resolution. The relative ease of obtaining high-resolution ^{13}C NMR spectra makes it the typical default nucleus for organic solid-state NMR spectroscopy. Nevertheless, the resolution of ^{13}C NMR spectra in the solid state is always inferior to that obtained in solution, and it is important to understand why this is so. In solution-state NMR, the resolution is generally

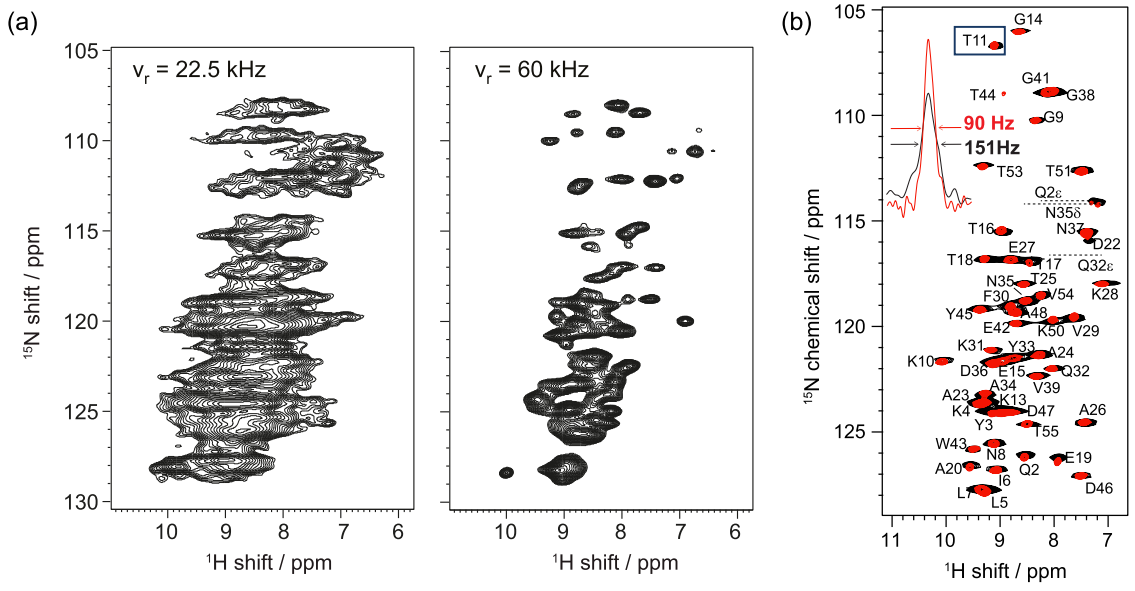

FIG. 1. (a) CP-HSQC spectra at 18.8 T (800 MHz ^{1}H NMR frequency) of a fully protonated sample of a single-stranded-DNA binding protein at MAS frequencies of (left) 22.5 kHz and (right) 60 kHz, respectively. Note the improvement in resolution in the ^{1}H dimension, which closely reflects the ratio of spinning rates. Adapted with permission from Andreas *et al.*, J. Magn. Reson. **253**, 36 (2015). Copyright 2015 Elsevier. (b) ^{1}H-detected ^{15}N-^{1}H CP-HSQC spectra of a fully protonated microcrystalline sample of the protein GB1 at MAS rates of 60 kHz (black) and 111 kHz MAS (red) at ^{1}H NMR frequency of 1 GHz. Adapted with permission from Andreas *et al.*, Proc. Natl. Acad. Sci. U. S. A. **113**, 9187 (2016). Copyright 2016 National Academy of Sciences.

limited by decay of the NMR signal due to spin-spin relaxation, characterised by the time constant T_2; indeed, in viscous solvents or for larger biomolecules, which tumble more slowly, T_2 typically becomes shorter, and linewidths increase. The relatively rapid decay of NMR signals in the solid state, however, is rarely determined by such relaxation. More typically, it is better described as a decoherence due to effects of dipolar couplings and/or dephasing due to inhomogeneous factors. Unlike incoherent decay due to relaxation, these are coherent mechanisms that can, in principle, be manipulated. Indeed, the absence of relaxation due to molecular tumbling can mean that the inherent resolution is higher in the solid state, particularly for quadrupolar nuclei, as described below.

There are a number of "inhomogenous" factors that broaden solid-state NMR linewidths and so reduce resolution. First, any deviation from crystalline symmetry means that different atoms in nominally the same environment will have different NMR frequencies. Hence disordered materials, such as glasses and polymers, will always have broad NMR lines, as discussed below. Second, powdered materials are generally not magnetically isotropic; different particle orientations will have different magnetic susceptibilities and hence different effective local magnetic fields. The resulting line broadening is only partially removed by MAS, and these susceptibility broadenings are often the limiting factor for spectral resolution in powdered samples, particularly where aromatic rings, and associated aromatic ring stacking, are present. An important feature of inhomogeneous broadenings is that they can be "refocused" by the application of spin-echo pulses (which is an appropriate point to note the great contributions of the late Erwin Hahn to NMR). Indeed, the term T_2' has been usefully introduced by Emsley and co-workers to describe the time constant for decay of magnetisation under spin-echo refocusing.[12] This is important in correlation experiments where relatively weak interactions, such as J coupling, are used to transfer coherence. Provided T_2' is sufficiently long, couplings can be used to transfer magnetisation *even though they are unresolved in the one-dimensional spectrum*. This is illustrated in Fig. 2, where the correlation peaks arise from ^{2}J coupling between ^{31}P nuclei in the same pyrophosphate unit in SnP_2O_7. The effective resolution of the 2D spectrum is much greater than that of the 1D MAS spectrum, allowing the number of distinct P sites to be determined and in turn constraining the possible space groups to which the structure could belong. Note that susceptibility-related shifts, for example, are identical for individual particles, and so the 2D spectra for samples where resolution is susceptibility limited are elongated along the diagonal;[13] such elongation of the peaks parallel to the diagonal is arguably present here. Analogous, but typically much stronger, effects are observed in 2D spectra of disordered materials, as discussed below.

In contrast to most inorganic systems, resolution in ^{1}H-containing systems is often limited by the residual effects of dipolar coupling to the ^{1}H spins. Although the couplings to the ^{1}H spin network are reduced by both MAS and by RF irradiation applied to the ^{1}H spins ("heteronuclear decoupling"), the effects of dipolar coupling are difficult to completely suppress and are often the limiting factor for the resolution of protonated sites, particularly CH_2 groups. This broadening is

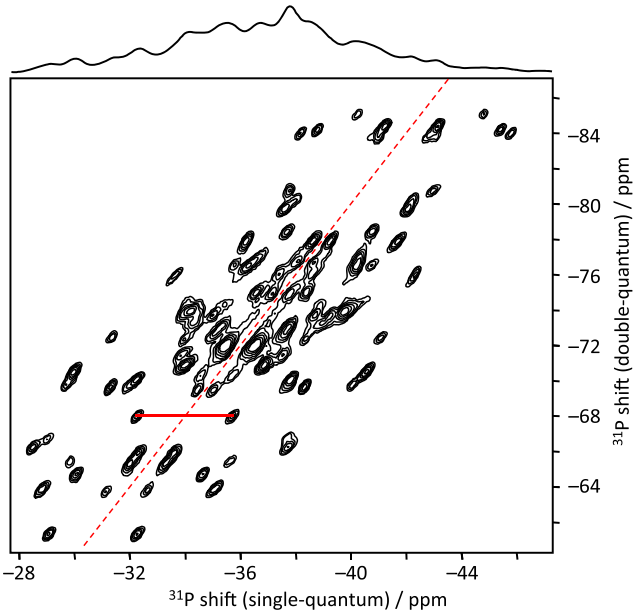

FIG. 2. ^{31}P double-quantum/single-quantum correlation spectrum of SnP_2O_7 obtained at 10 kHz MAS using the refocused INADEQUATE experiment. Peaks either side of the diagonal (red dashed line) connect pairs of ^{31}P within the same $[P_2O_7]^{2-}$ unit which are correlated via a ^{2}J coupling (one pair highlighted with red line). The MAS spectrum is shown above. Adapted from Ref. 11.

"homogeneous" in the sense that it is not refocused by a spin echo. The design and optimisation of pulse sequences for heteronuclear decoupling has provided an important and on-going challenge in solid-state NMR research. A major part of the challenge lies in the fact that the various interactions (including the dipolar couplings) are of a similar order of magnitude to the MAS rates (10–15 kHz) and RF nutation rates (50–80 kHz) typically used in routine ^{13}C solid-state NMR. This generates a variety of "resonance conditions," with significant effects on decoupling performance. Moreover, as noted above, experimental features, such as non-uniform RF fields, also have a significant effect on performance, and the effectiveness of sequences with multiple parameters can be very sensitive to how these are optimised. Although the overall theoretical picture of heteronuclear decoupling is now well established,[14–16] the long coherence life-times that can be achieved with optimised decoupling, ironically, make it difficult to develop good quantitative models of decoupling performance.[17] In practice, however, it is generally straightforward to obtain good results with a minimum of optimisation, particularly when resolution is limited by inhomogeneous factors. Optimisation is more important where T_2' is the limiting factor, e.g., in correlation experiments; see Ref. 18 for a recent overview. Note that under ultra-fast MAS conditions, it is often advantageous to work in a "low-power" decoupling regime where the RF decoupling is "tidying up" after the averaging effects of fast MAS. Indeed, particularly for samples in which the ^{1}H coupling network has been diluted by deuteration, it is often appropriate to use decoupling sequences developed for solution-state NMR.[19]

For nuclei with spin quantum number $I > 1/2$, NMR spectra are additionally affected by an interaction between the nuclear quadrupole moment (not present when $I = 1/2$) and

the electric field gradient (EFG) acting at the nucleus.[1–3,20] As the resulting broadening depends on the magnitude of the quadrupolar moment (Q), nuclei with small Q, such as ^{2}H, ^{6}Li and ^{133}Cs, are typically much easier to observe experimentally. However, the EFG is very strongly dependent on the atomic-scale chemical environment, and so the overall magnitude of the quadrupolar coupling (C_Q) varies significantly, from just a few Hz for species in symmetric environments to tens of MHz in other cases. In practically relevant systems and at reasonable magnetic field strengths, the interaction remains smaller than the Zeeman interaction, and its effect can be described by a perturbation to the Zeeman energy levels. To a first-order approximation, this lifts the degeneracy of the $2I + 1$ allowed (i.e., single-quantum) transitions, and although these can be measured individually for a single crystal, the dependence on orientation of the quadrupolar interaction results in a significant spectral broadening for a powdered sample. For quadrupolar nuclei with a half-integer spin quantum number (i.e., 3/2, 5/2, etc.), the so-called central transition (CT) between the $m_I = +1/2$ and $m_I = -1/2$ levels is unaffected by this interaction, leading to spectra that contain a sharp central transition (CT) and broadened satellite transitions (STs). In this case, it is usual to acquire spectra that contain only the CT signal and neglect the much broader ST, unless C_Q is particularly small. The quadrupolar interaction to first order (with respect to the Zeeman interaction) is still described by a rank 2 tensor meaning that it can be removed using MAS; however, owing to its magnitude, the challenge can often be achieving sufficiently rapid rotation rates. This typically leads to spectra that contain manifolds of spinning sidebands rather than a single, isotropic line for each distinct site. The relative sideband intensities, however, encode information on the anisotropy of the local EFGs, and so can provide useful insights into the symmetry of the coordination environment.

In some cases, the magnitude of the quadrupolar interaction means that a second-order perturbation must be considered. This results in rank 2 and rank 4 anisotropic contributions to the frequency of all transitions (including the CT for half-integer spins) and an isotropic (rank 0) term. This more complex orientation dependence means that MAS is ineffective in removing completely the quadrupolar broadening and results only in a narrowing of the powder-pattern line shapes. For samples with multiple distinct species present, this limits the resolution and can prevent the extraction of site-specific information. This can be seen in the ^{27}Al MAS NMR spectrum of a calcined microporous phosphate framework (AlPO-14) in Fig. 3(a), where signals from the expected four Al species cannot be resolved. The acquisition of high-resolution spectra for quadrupolar nuclei has been the focus of intense research for the last 3–4 decades and has resulted in a number of different approaches. Earlier methods used composite sample spinning techniques in an attempt to average both the rank 2 and rank 4 contributions by physical manipulation of the sample. This led to the development of double rotation (DOR),[21] where a smaller rotor is rotated at an angle of 30.56° (to average the rank 4 term) inside a second rotor, inclined at 54.74°, and dynamic angle spinning[22] (DAS), where rotation around two different angles is performed sequentially. The technical challenges of these techniques, and the need for expensive and specialist hardware, has limited their widespread use. The most popular current approaches for high-resolution experiments use an entirely different philosophy, combining the correlation of different transitions within the spin system (or the so-called "spin-space" averaging) to remove rank 4 broadening, with MAS

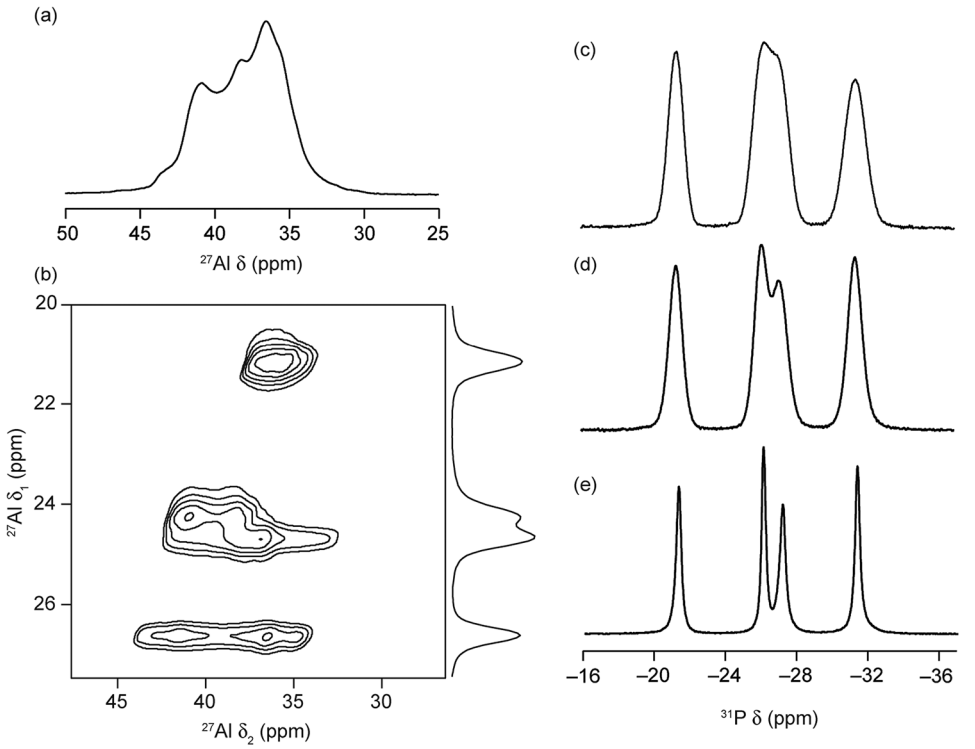

FIG. 3. ^{27}Al (14.1 T) (a) MAS and (b) MQMAS NMR spectrum of calcined AlPO-14. ^{31}P (14.1 T) MAS NMR spectra of calcined AlPO-14 acquired (c) without any decoupling, (d) with continuous wave ^{27}Al decoupling, and (e) with multiple pulse ^{27}Al decoupling.

to remove the rank 2 contribution. The resulting multiple-quantum MAS (MQMAS)[23,24] and satellite-transition MAS (STMAS)[25,26] experiments correlate multiple-quantum (e.g., $m_I = +3/2 \leftrightarrow m_I = -3/2$) and satellite transitions, respectively, with the CT. Despite the much greater sensitivity of STMAS, the more significant technical challenges associated with its practical implementation (including extremely accurate setting of the spinning angle and a very stable rotation rate) have resulted in MQMAS being widely adopted as the method of choice, and considerable research effort has been invested in improving its sensitivity. Figure 3(b) shows the ^{27}Al MQMAS spectrum of calcined AlPO-14, where the four Al species can be clearly resolved, and the NMR parameters for each site are now easily extracted.[27]

The inherently quantitative nature of most NMR spectra, with spectral intensities directly reflecting the relative proportions of each species present in the sample, is one of its most useful features. For quadrupolar nuclei, however, the dependence of the nutation rate on the magnitude of C_Q means that maximum signal intensity is rarely observed for different species at one RF pulse duration.[28] To overcome this problem, it is possible to correct the relative intensities measured experimentally by comparison to simulation, or to acquire spectra using a very short pulse duration. Although many quadrupolar nuclei are present exclusively in inorganic materials (where ^{1}H are typically not present, or ^{1}H spin networks are more dilute), it may be necessary to apply decoupling (typically of ^{1}H or ^{19}F), particularly in MQMAS experiments where narrow spectral lines are obtained. Similarly, coupling to nearby quadrupolar spins can have a deleterious effect on the spectral resolution of spin $I = 1/2$ nuclei. Lines can be narrowed either by applying low-power RF pulses to the quadrupolar spin during spectral acquisition (avoiding any resonance conditions with the MAS rate, as described earlier) or, as shown more recently, by using multiple pulses ideally *not* synchronised with the rotor period.[29] This is shown in Figs. 3(c)–3(e), for calcined AlPO-14, where resolution of the four distinct species in the ^{31}P MAS NMR spectrum is improved by low-power continuous wave decoupling, but the highest resolution is obtained when multiple-pulse decoupling is applied.

III. EXPLOITING RESOLUTION FOR NMR CRYSTALLOGRAPHY

Although NMR spectra can always be used as fingerprints of distinct solid forms, e.g., to distinguish different crystalline organic polymorphs by their ^{13}C NMR spectra, it is often difficult to relate individual chemical shifts to structural features. Indeed, even with excellent resolution, it can be challenging to assign the signals observed to a given chemical environment, particularly in structures with multiple distinct molecules per formula unit in the basic asymmetric unit ($Z' > 1$). This is a particular challenge for inorganic solids, as many more (and less common) nuclear species are typically investigated, and much less information has been collated in the literature in comparison to ^{1}H and ^{13}C NMR of small molecules. The ability to predict NMR parameters from first principles for a given structural model has contributed to the emergence of a developing field, usually referred to as NMR crystallography,[30–33] recognised as an International Union of Crystallography commission in 2014.[34] In this area, NMR is used to solve or refine structures in combination with information from diffraction and, in many cases, computation. Although quantum-chemical calculations have been used to predict NMR parameters for many years, extended solids were typically modeled as a large molecule or cluster, leading to problems both with the termination of bonds (and consequent perturbation of the local structure) and with the size of the system necessary to produce accurate results. The introduction of calculation methods employing periodic boundary conditions, i.e., which exploit, rather than avoid, the periodic nature of the solid state, revolutionised the application of computation in solid-state NMR spectroscopy.[35,36] Although often employed to aid spectral assignment, calculations can also be used to explain any unusual spectral line shapes that are observed and as support for the accuracy of the parameters extracted from experimental spectra. In cases where sensitivity causes problems for an experimentalist, calculations can predict NMR parameters in advance and guide practical measurement. The ease with which geometric parameters (such as bond distances and bond angles) can be varied within a calculation provides a convenient and extremely powerful approach for understanding the dependence of NMR parameters on the local environment.

The vast majority of modern calculations exploit density functional theory (DFT),[37] where the total energy of a system is expressed as a function of the electron density, and all properties can be derived from this. Most contributions to the total energy are known exactly, but the term describing the inter-electron interactions (the exchange-correlation contribution) must be approximated. This has resulted in a range of different functionals, many optimised for particular systems, but those based on the generalized gradient approximation (GGA) have found significant success for predicting solid-state NMR parameters. In many cases, periodic DFT is combined with a plane wave basis set, with the accuracy of the calculation determined both by the kinetic energy cutoff of the plane waves that are considered and the number of points used to sample the first Brillouin zone in reciprocal space. Computation of the quadrupolar NMR parameters is relatively straightforward, as the EFG is a function solely of the total charge density, while the shielding tensor requires the response of the electrons to a magnetic field to be calculated. For comparison to experiment, it is usually necessary to convert the computed isotropic shieldings into chemical shifts. Despite the difference in conditions (DFT calculations implicitly predict properties at 0 K), excellent correlation between calculation and experiment has been shown for many nuclei, e.g., ^{13}C and ^{29}Si, although in other cases (notably for ^{19}F) computational shifts sometimes have to be "scaled" to provide a better match to experiment and so facilitate spectral interpretation.[33,36,38] More recent developments have also enabled J couplings to be calculated for periodic systems.[39] These have also found application in the study of the interactions that affect crystal packing in the solid state, including hydrogen bonding[40] and unusual "through space" J couplings.[41,42] Recent work has shown that hybrid functionals (which incorporate a portion of exact exchange from Hartree-Fock theory) can improve the prediction of

solid-state properties. Although their implementation is expensive in plane wave codes, they can be usefully employed to predict NMR parameters in fragment-based approaches and have shown promising results for ^{13}C chemical shifts of molecular organic crystals.[43] In general, calculations provide information on the full interaction tensor, with the principal components (and the corresponding derived NMR parameters) obtained after diagonalisation. This is a considerable advantage for the experimentalist, as anisotropic information can have a significant effect upon NMR spectra (and therefore might be relevant in, for example, analytical fitting), but can be difficult to measure easily or accurately, particularly under MAS.

In order to predict NMR parameters, an initial structural model is required. These can be obtained from prior computational work, but in many cases are derived from crystallographic diffraction. The accuracy and relevance of the model will depend upon whether the experimental measurement was made on a single crystal or a powdered sample or whether X-ray, synchrotron, or neutron data were used. The exquisite sensitivity of NMR parameters to the local structure means that it is often necessary to "optimise" a structural model prior to calculating NMR parameters, minimising forces upon the atoms.[20–24] This can be of particular importance for H positions estimated from X-ray diffraction data. For example, Yates *et al.* showed that for flurbiprofen, mean differences between experimental and computed ^{13}C chemical shifts improved from 5.5 ppm to 2.7 ppm upon DFT optimisation of the H positions and to 2.5 ppm when the coordinates of all atoms were allowed to vary.[44] Indeed, the difficulty of locating H atoms in XRD studies means that NMR crystallography can be an effective means of identifying incorrect structures; see, for example, Ref. 45 and references therein. For many molecular systems, optimization of atomic coordinates (either of H or of all atoms) is typically carried out with lattice parameters fixed at their values determined by diffraction. However, optimization of the lattice parameters can also provide improved agreement with experiment, as demonstrated by Ashbrook *et al.*[27] for ^{27}Al and ^{31}P NMR parameters for the microporous aluminophosphate, AlPO-14, where optimisation changed the proposed assignment of the ^{31}P MAS spectrum. Full optimization should be carried out with some caution, however, as failure to include dispersion interactions can produce inaccurate results, as demonstrated in Refs. 20–24. This has been tackled in recent code developments by the introduction of semi-empirical dispersion correction (SEDC) schemes (which can be used in conjunction with standard density functionals and are able to reintroduce the effect of the attractive forces between atoms that result from long-range correlation effects) such as the D2 scheme by Grimme.[46] Better agreement with experiment was nicely demonstrated by Dudenko *et al.*,[47] in the study of an organic co-crystal; DFT optimization using only a GGA functional resulted in an expansion of the unit cell by ~19%, while the inclusion of an SEDC scheme produced a much smaller change (a contraction of ~3%–5%). Similarly Sneddon *et al.* obtained much better agreement between experimental XRD measurements and DFT optimized structures when SEDC schemes were employed for AlPO materials, although there was a much smaller difference between the calculated NMR parameters for structures optimised with or without dispersion.[48] Another potential cause of concern, flagged above, is that NMR crystallography approaches generally involve DFT calculations predicting properties at 0 K based on crystal structures frequently obtained between 100 and 120 K and comparing the results to NMR experiments performed at ambient temperature! It has been shown, however, that isotropic chemical shifts, and particularly relative isotropic chemical shifts, are not significantly affected by the small-angle libration-type processes typical of motion in the solid state,[49] and comparisons between experimental and calculated shifts are, in most cases, limited by the intrinsic approximations of DFT rather than the effects of finite temperature.

If a structural model is not available, it may be possible to generate an initial starting point by manually modifying a model for a related material followed by accurate optimization. If this is not an option, it may be necessary to generate models using approaches based on crystal structure prediction (CSP), with recent NMR crystallography work exploiting the CSP methods of Day[51] and the *ab initio* random structure searching (AIRSS) method of Needs and Pickard.[52] CSP has been shown to be particularly useful for molecular systems, with candidate structures generated by Monte Carlo simulated annealing of pre-optimised molecular conformations in common space groups and then optimized and ranked by energy before NMR parameters calculated for relevant structures are compared to

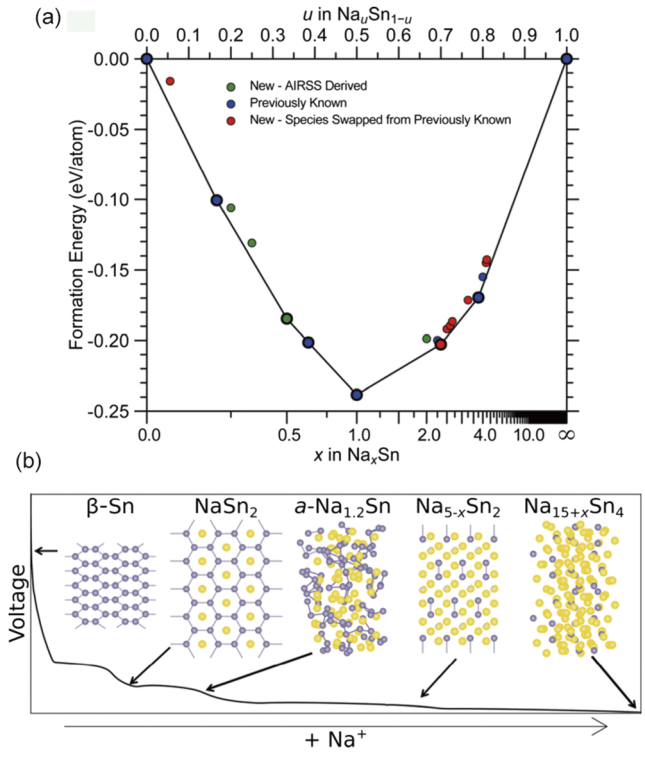

FIG. 4. (a) Plot of formation energy per atom in potential Na–Sn based anode materials as a function of composition. Blue points denote previously known structures, those in green were found using AIRSS, and the red points denote new materials obtained by swapping atomic species from other known phases. (b) Schematic showing the likely Na–Sn structures formed during electrochemical cycling of a Na–Sn cell, as the Na content increases. Adapted from Stratford *et al.*, J. Am. Chem. Soc. **139**, 7273 (2017). Copyright 2017 Authors, published under a Creative Commons Attribution (CC-BY) license.

experiment. Work by Emsley and co-workers demonstrated the feasibility of this approach in an NMR-crystallographic structure solution of thymol, although interestingly comparison to NMR spectra was shown to be vital in elucidating the correct structure, as this was only the third lowest in energy.[53] The AIRSS approach produces a large number of candidate structures using randomised unit cell parameters and atomic coordinates, which are subsequently optimised using DFT. Although in principle the number of structures that can be searched is restricted by the higher cost of DFT (in comparison to cheaper force-field approaches), the unbiased nature of the method has significant advantages for inorganic systems and for predicting higher-energy (but perhaps still experimentally relevant) structures. AIRSS has been combined with the calculation of NMR parameters to study battery materials (e.g., identifying the structure of previously-unknown structures of Li/Ge phases[54]), silicate minerals (e.g., locating the position of H in high-pressure materials of relevance in the inner Earth[55]), and organic molecules (e.g., to study possible polymorphism[56]). Figure 4 shows the energy of AIRSS-predicted structures of potential Na–Sn based anode materials as a function of composition. Comparing calculated NMR parameters to those from *in operando* experimental measurements allowed the materials present during electrochemical cycling to be identified.

IV. BEYOND PERIODICITY

Periodic symmetry means that corresponding sites in different crystallographic unit cells have the same NMR frequencies, making it more likely to obtain well-resolved spectra with respectable sensitivity. Periodicity also facilities efficient plane wave DFT-based calculations, as discussed above. One of the principal attractions of NMR, however, is that it does not require long-range order and hence is applicable to a broader range of materials than, for example, Bragg diffraction-based studies. In this section, we consider the effects of "disorder" on solid-state NMR and approaches to optimising sensitivity and resolution in such systems.[57,58]

In contrast to diffraction-based methods, there is a clear distinction in NMR studies between "static" disorder, e.g., glassy materials with distributions of local structures and "dynamic" disorder due to thermal motion. Different types of disorder are illustrated in Fig. 5. Figure 5(a) shows the ^{89}Y spectra of a series of $Y_2Ti_{2-x}Sn_xO_7$ pyrochlores[59] as a function of Sn composition x. The Y sites have 6 next nearest neighbour sites that can be occupied by either Sn or Ti. The NMR spectra of materials with $0 < x < 1$ clearly show that a distribution of local environments are present. Figure 5(b) shows calculated ^{89}Y shifts as a function of the local substitution pattern, confirming that the different peaks observed largely correspond to the numbers of Sn vs. Ti next nearest neighbours. It is not always the case that distribution of local environments can be observed so directly from the NMR spectrum; indeed the corresponding ^{119}Sn spectra vary with x in a much less obvious way, but one that could be rationalised with the aid of calculations.[60] Alternative characterisation techniques would not be able to show that Sn/Ti substitution was random in such a visually direct fashion.

The spectra of statically disordered materials generally exhibit lower resolution than those of ordered materials; in the typical case where the broadening due to disorder exceeds the intrinsic linewidth, the broad line shape provides direct information about the distribution of chemical environments. Crucially, disordered materials prepared by different routes may have distinct NMR spectra despite showing indistinguishable amorphous "halos" in diffraction experiments. The site-level information provided by NMR can help understand the molecular origins of such "polyamorphism."[63] Two-dimensional techniques are particularly powerful in this context since 2D spectra will reveal correlations between the distributions. This is illustrated in Fig. 5(c) using a ^{29}Si double-quantum/single-quantum correlation experiment (refocused INADEQUATE) on a surfactant-templated layered silicate.[61] The one-dimensional MAS spectrum shows the broad non-uniform features typical of a statically disordered system. The line shapes of the 2D spectrum, however, are surprisingly narrow, indicating that the frequency distributions in adjacent sites are strongly correlated. The resolving power and sensitivity of the 2D spectrum is thus significantly higher than would be expected from the MAS spectrum. Note that, as in Fig. 2, the refocused INADEQUATE spectrum uses J couplings to establish correlations, even though these not resolved in the 1D spectrum. Moreover, the dependence of J couplings on features such as bond angles means that measurements of couplings using spin-echo experiments can provide valuable insights into challenging structures such as incommensurate frameworks.[64]

Lack of periodicity makes quantum chemical calculations on disordered systems more challenging. In the pyrochlore example above, a single unit cell was sufficient to model the distribution of NMR shifts. Obtaining suitable structural models is more of an open research question for glassy-type disorder and polymeric materials. Approaches that have been used successfully in NMR studies include quench-cooling of MD simulations of molten solids,[65] as well as approaches that avoid the need for large-scale DFT calculations, such as training neural networks to predict chemical shifts in glasses[66] or deriving empirical correlations from related compounds.[67,68]

In contrast to "static disorder," dynamics tend to average NMR parameters, and so, depending on the time scale of the dynamics, will narrow rather than broaden NMR line shapes. This is illustrated in Fig. 5(d), which shows the ^{23}Na spectrum of Na-doped $SrSiO_3$. Based on their high ionic conductivities, these materials had been proposed as oxide ion conductors for solid-oxide fuel cells. Crucially, however, the bulk conductivity measurements could not identify the origin of the ionic conductivity. The broad asymmetric line shape of the ^{23}Na spectrum at low temperature is characteristic of a glassy solid, while its evolution to a narrow Lorenztian line shape is indicative of dynamic hopping between the available sites until a single averaged frequency is observed. Although NMR experiments at such elevated temperatures require specialist probes, the direct visual insight they provide is unparalleled. This example involved a static sample since magic-angle spinning would not have provided additional resolution or sensitivity. Obtaining MAS spectra outside the predicted

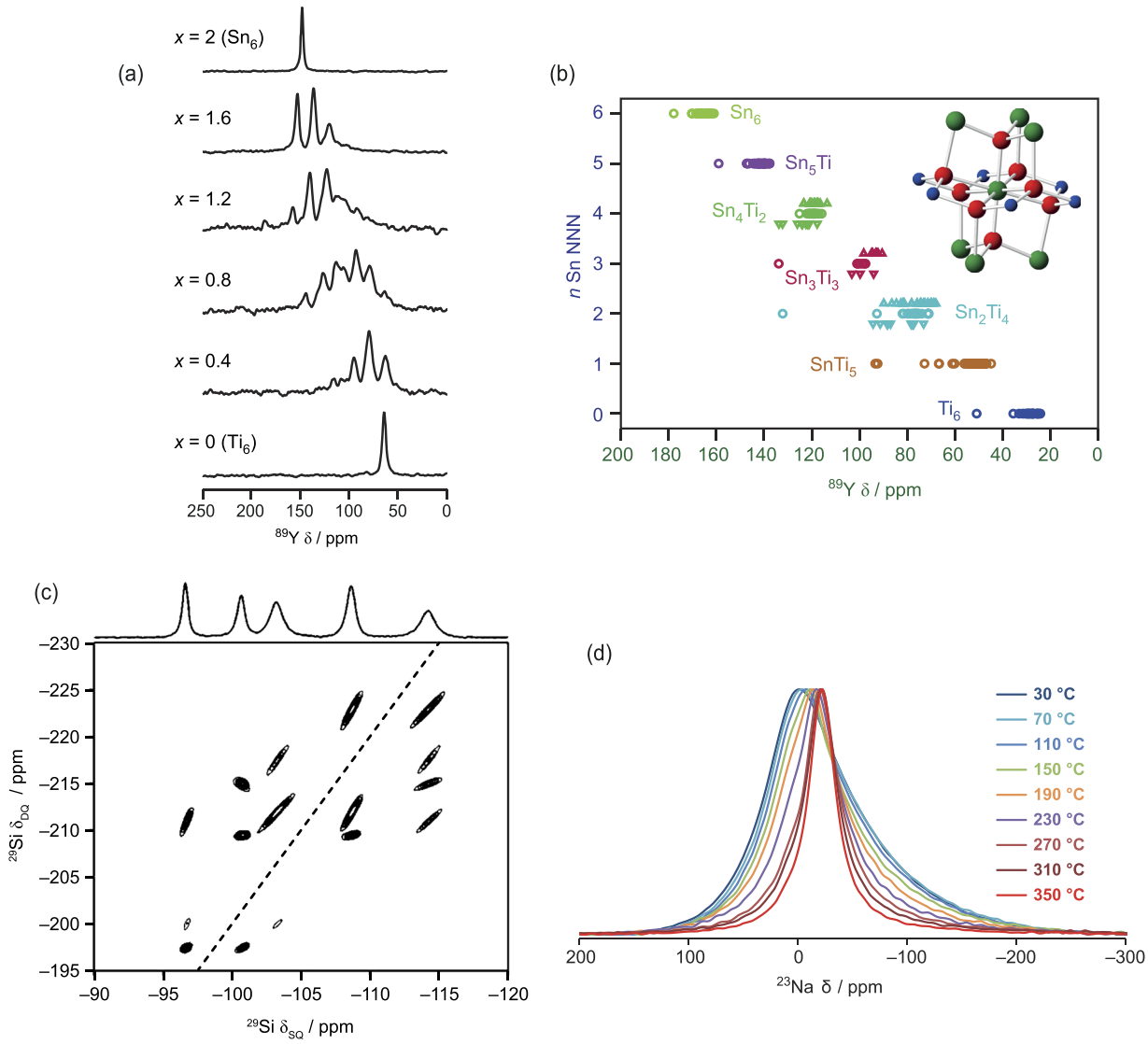

FIG. 5. (a) ^{89}Y MAS NMR spectra of $Y_2Ti_{2-x}Sn_xO_7$ pyrochlores, (b) local environments of the A (Y, green) and B (Sn/Ti, blue) cations within the pyrochlore structure (O atoms shown in red) and plot of calculated ^{89}Y isotropic chemical shifts for different Sn/Ti substitutions of the surrounding B site cations. (c) ^{29}Si/^{29}Si double-quantum (INADEQUATE) correlation spectrum of a surfactant-templated layered silicate. (d) ^{23}Na NMR spectra of a Na-doped strontium silicate sample of nominal composition $Sr_{0.6}Na_{0.4}SiO_{2.8}$ as a function of temperature (peak heights normalised). Adapted from Refs. 59, 61, and 62, respectively.

range of typical commercial NMR probes (typically −100 to +200 °C) is quite challenging. The development of Dynamic Nuclear Polarisation (DNP) methodology (see below) has, however, generated new interest in obtaining MAS spectra at low temperature (DNP enhancement is generally performed at ∼90 K). Although freezing out molecular motions has drawbacks in terms of reducing motional line-narrowing and lengthening relaxation times (and hence repetition periods), MAS at cryogenic temperatures does allow low-temperature phenomena, such as superconductivity,[69] to be explored by NMR.

It is not only NMR linewidths that are sensitive to dynamic processes; different NMR observables allow dynamics to be explored over a wide range of frequency scales. For instance, very slow processes (limited only by nuclear relaxation times, which are typically seconds or longer) can be studied via magnetisation exchange experiments, while fast motions (of the order of nanoseconds) modulate the spin-lattice relaxation times themselves, as these are sensitive to motion on the order of the NMR Larmor frequencies. Intermediate time scales can be accessed via spin-lattice relaxation in the rotating frame of reference, $T_{1\rho}$, which is sensitive to motion of the time scale of RF nutation frequencies, while ^{2}H NMR has been widely used where isotropic substitution is feasible. Given the vast scope of the literature,[70–73] we just present here some illustrative examples and indicate ongoing challenges.

As noted, ^{2}H NMR has been widely used to study dynamic processes in molecular organic systems.[75] The ^{2}H EFG tensor in X–H bonds is symmetric and aligned with the X–H bond vector to an excellent approximation. Hence, measuring the ^{2}H quadrupolar coupling parameters provides direct insights into the re-orientation of individual bonds. The ^{2}H quadrupole moment is sufficiently small that ^{2}H NMR spectra

can be obtained readily with standard techniques, while different experiments can be used to measure dynamics in slow, fast, or intermediate time scales. In many problems of interest, e.g., probing H sites involved in hydrogen bonding or the dynamics of included solvent, isotopic substitution with ^{2}H is straightforward and relatively inexpensive. Particularly when allied with MAS, ^{2}H NMR can be used to probe complex behavior, such as water motion and H exchange in pharmaceutical hydrates.[76] Isotopic enrichment is not always feasible, and so it is useful to be able to obtain information on dynamics via "dilute" spins, such as ^{13}C. (Although ^{1}H NMR relaxation and times and linewidths can provide valuable information on overall dynamics, the "spin diffusion" due to the strong dipolar interactions between ^{1}H spins makes it difficult to localise the molecular origins of the results observed.) Figure 6 illustrates two applications of ^{13}C NMR for characterising dynamics. Figure 6(b) plots the temperature dependence of the ^{13}C T_1 relaxation times for protonated carbons on the furan rings of the drug furosemide (FS) in a co-crystal form with isonicotinamide. The relaxation is largely driven by dipolar interactions to the bonded ^{1}H nuclei, and so fitting the "T_1 minimum" curves provides the thermal activation parameters for the reorientation of the furan rings. The activation parameters of the two distinct furan rings in the crystal asymmetric cell are indistinguishable and are both consistent with a small amplitude libration-type motion. This contrasts with the starting model provided by X-ray diffraction, Fig. 6(a), in which one furan ring is modeled in terms of a large amplitude ~180° disorder, but the other is not. Analysis shows that the X-ray diffraction data cannot readily distinguish between large and small amplitude disorder, i.e., the NMR data is required to show that the two rings have essentially the same dynamics. At the other end of the frequency spectrum, Figs. 6(c) and 6(d) illustrate the use of ^{13}C NMR to probe slow re-orientational jumps in a polymeric system. The "CODEX" experiment is sensitive to re-orientation of the ^{13}C CSA anisotropy tensor, and the simulated curves are consistent with an effective re-orientation angle of 103° predicted on the basis of defects travelling along the polymer chain.

In terms of future perspectives, the progress in obtaining high-resolution spectra from biomolecular solids illustrated above in Fig. 1 will facilitate the study of dynamics in proteins and other biopolymers. This will be particularly advantageous for probing dynamics via relaxation times since the relaxation in the solid state is not complicated with relaxation due to overall molecular motion, as is the case in solution. A drawback of using relaxation times to probe dynamics is that it is generally difficult to infer the type of motional process from

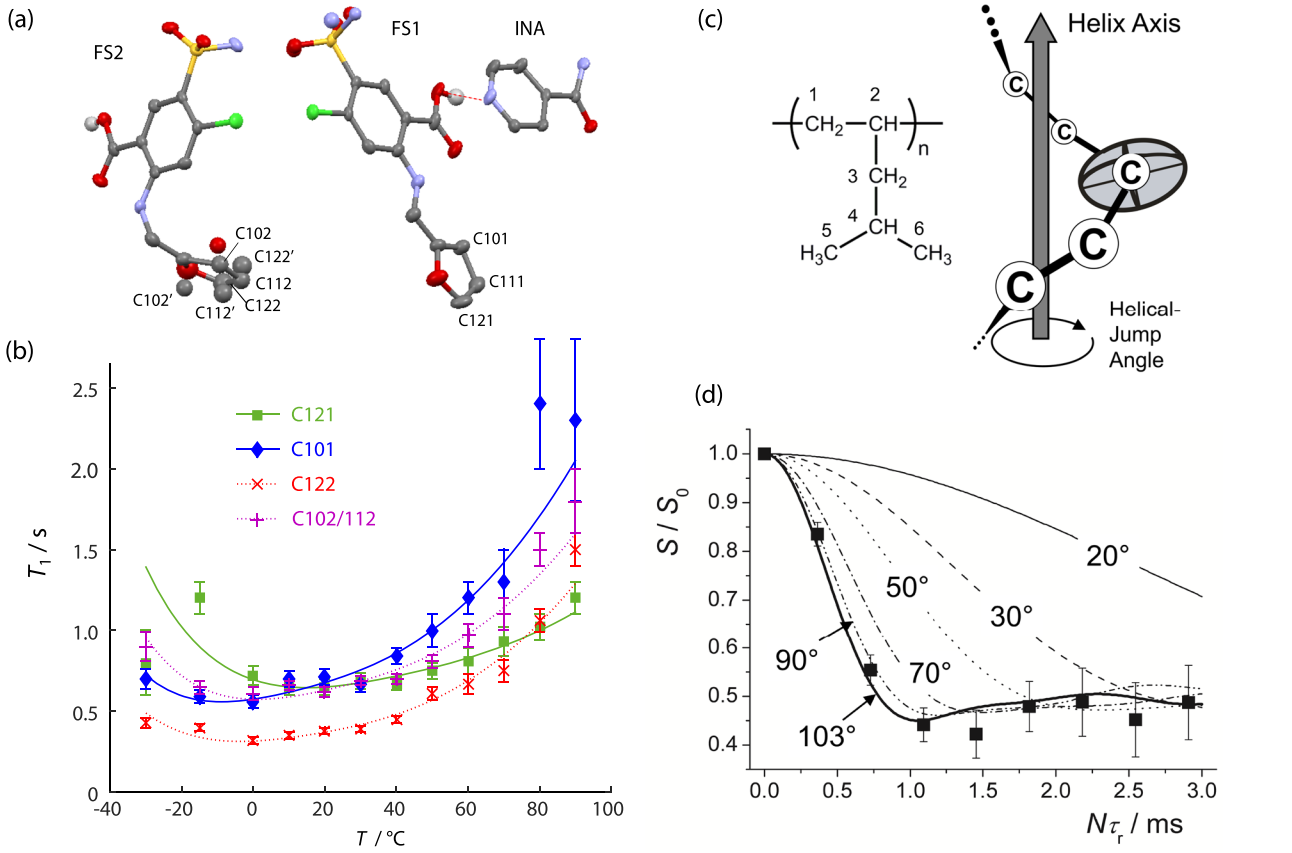

FIG. 6. (a) Asymmetric unit of a furosemide (FS)-isonicotinamide (INA) co-crystal, with the carbon labeling of the FS furan rings shown. The ring on FS2 was modeled as disordered over two positions (alternate position distinguished with '). (b) Temperature dependence of the ^{13}C T_1 relaxation times for the furan carbon atoms, together with fits for a simple motional model. Adapted from data published in Ref. 74. (c) Monomer unit and schematic representation of the helical main chain of poly(4-methyl-1-pentene), P4M1P, illustrating the helical jump angle. The ellipsoid represents a CSA tensor, whose re-orientation is monitored by the CODEX experiment. (d) Experimental CODEX results (symbols) for the C1 carbon of P4M1P and calculated (lines) for different helical jump angles. From Reichert and Krushelnitsky, *Modern Methods in Solid-State NMR: A Practitioner's Guide*. Copyright 2018 The Royal Society of Chemistry. Reproduced with permission from The Royal Society of Chemistry.

the NMR data, e.g., T_1 minima in Fig. 6(b) would be equally well fitted by various motional models. We expect that molecular dynamics simulations and related techniques will have a significant role to play in linking molecular-level behavior with NMR observables.[77]

V. SENSITIVITY ENHANCEMENT

The inherently poor sensitivity of NMR spectroscopy, resulting from the low Boltzmann population differences between the nuclear spin energy levels, provides an ongoing challenge. Simple solutions include lowering the temperature (although this can be technically difficult when rapid sample rotation is also required) and increasing the external magnetic field strength, as sensitivity is proportional to $\sim B_0^{3/2}$.[3] This latter approach is particularly useful for low-γ nuclei and has an additional advantage for quadrupolar nuclei, as it also provides a line narrowing (and therefore a further increase in sensitivity), as the second-order quadrupolar broadening is proportional to B_0^{-1}.[20] More generally, any line narrowing method will also improve the signal-to-noise ratio in a spectrum; however, the fast MAS often employed to average larger interactions restricts the sample volumes that can be studied, limiting the sensitivity obtained. For nuclei with particularly low natural abundance (e.g., ^{2}H, ^{13}C or ^{17}O), it is also possible to improve sensitivity by isotopic enrichment. This can be carried out at an early stage in a synthetic procedure, post synthesis on the final product, or during a reaction of interest. While enrichment offers significant sensitivity gains (and concomitant time savings), it often poses a considerable experimental challenge, requiring the development of cost- and atom-efficient synthetic procedures, owing to the typically high cost of isotopically enriched reagents. For example, for ^{17}O (natural abundance 0.037%), methods that minimize the amount of $H_2{}^{17}O$ required in a synthesis or reaction, such as dry gel conversion methods, ionothermal reactions, or the use of very low reaction volumes, have been employed to reduce the cost of producing enriched material.[78–81] In addition to the improvement in sensitivity, enrichment has further advantages, including the possibility to utilize other interactions (such as the ^{2}H quadrupolar interaction to study dynamics, as discussed above) or the use of selective enrichment to aid spectral assignment[82,83] or simplify complex spectra of biomolecules.[83]

It is also possible to improve the efficiency of many NMR experiments by careful choice/optimisation of the RF pulse sequence used. One common approach is cross polarisation (CP),[85] which involves the transfer of magnetisation from one spin (I, typically with high γ and high natural abundance) to a second spin (S, usually with lower natural abundance and lower γ). The maximum possible gain in sensitivity is proportional to γ_I/γ_S, i.e., a factor of four for ^{1}H and ^{13}C. A further gain per unit time can typically be realised as the repetition rate in a CP experiment is governed by the relaxation rate of the abundant spin, which is typically much faster than that of a dilute spin. CP transfer proceeds via the dipolar interaction (and so is proportional to $1/r^3$), offering information on spatial proximities and the ability to edit spectra simply on the basis of internuclear distances. While extremely useful for nuclei with spin $I = 1/2$, the spin dynamics governing CP to quadrupolar nuclei are considerably more complex,[86–89] with the efficiency additionally dependent on the quadrupolar parameters, the RF field strength and the MAS rate. A sensitivity enhancement is often not observed, although CP remains useful for spectral editing or magnetisation transfer within two-dimensional experiments. The ability to transfer magnetisation between spins, using techniques such as CP, also enables sensitivity enhancement via indirect detection; i.e., the addition of a final step to an experimental sequence that transfers magnetisation to a different spin with higher γ, typically ^{1}H, to exploit the greater efficiency of signal detection at the higher frequency. An example is shown in Fig. 7, which show ^{1}H-detected ^{15}N spectra of a small polypeptide alongside corresponding ^{15}N CP MAS spectra [note that the ^{15}N/^{1}H spectrum in Fig. 1(b) was also acquired using inverse detection]. The indirectly detected spectrum acquired at 40 kHz MAS shows comparable signal-to-noise to the conventional 1D spectrum but has the advantage of providing additional correlation information, while the indirectly acquired spectrum at 80 kHz MAS has much better S/N than the 1D spectrum. As seen, very fast MAS rates are required to narrow ^{1}H linewidths for inverse detection to be effective. The associated limitation on sample volumes is, however, an advantage for such isotopically enriched biomolecular systems, where the production of significant sample volumes is both difficult and expensive.

An additional approach for sensitivity enhancement involves the use of CPMG (Carr Purcell Meiboom Gill) echo trains.[90,91] This involves applying a series of inversion pulses throughout acquisition, resulting in a free-induction decay (FID) that contains a series of echoes, which, upon Fourier transformation, break up the spectral line shape into a series of "spikelets." This provides a significant improvement in the peak height signal-to-noise ratio. For quadrupolar nuclei, techniques such as CPMG are often combined with the prior manipulation of the populations of the nuclear spin energy levels, thereby increasing the population difference across the CT before the NMR pulse is applied. A number of approaches aimed at inverting the population of the STs have been developed,[92] involving frequency sweeps [as in double-frequency sweep (DFS)], adiabatic pulses (such as hyperbolic secant or HS pulses), or phase-alternated pulses, as in rotor-assisted population transfer (RAPT) or fast amplitude modulation (FAM). The relatively poor sensitivity of the popular MQMAS experiment for acquiring high-resolution NMR spectra of quadrupolar nuclei has also been the focus of much attention. In particular, the use of a single pulse for the conversion of multiple-quantum coherences within the experiment is typically inefficient, and many approaches have replaced this pulse with more sophisticated composite pulses. Impressive enhancements (e.g., factors of 2-3) have been achieved using DFS[93] and FAM[94] pulses, with recent work in this area employing an automated computational optimisation of FAM pulses (or the FAM-N[95,96] approach). This latter approach gives experimental pulses which are robust to small variations in nutation rate and C_Q, and that can be used without further optimisation, making them applicable to a wide range of materials.

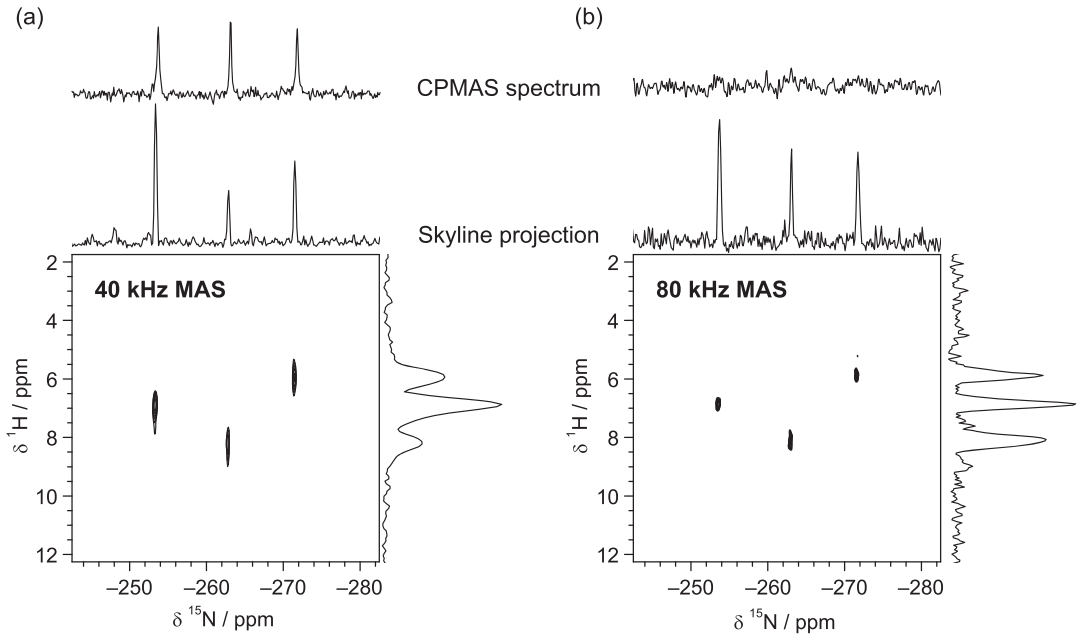

FIG. 7. ^{1}H-detected 2D heteronuclear correlation (HETCOR) spectra of the tripeptide *N*-formyl-L-methionyl-L-leucyl-L-phenylalanine-OH obtained at 14.1 T at MAS rates of: (a) 40 kHz (1.6 mm rotor, sample volume 6 μL) and (b) 80 kHz (1.0 mm rotor, sample volume 0.8 μL). Skyline projections of the 2D spectra are compared with the 1D CPMAS spectra normalized to the same noise level. All experiments had the same duration (5 h). From Kobayashi *et al.*, *Modern Methods in Solid-State NMR: A Practitioner's Guide*. Copyright 2018 The Royal Society of Chemistry. Reproduced with permission from The Royal Society of Chemistry.

There has been considerable recent interest in improving the sensitivity of NMR spectroscopy by transferring polarisation from electrons using DNP.[97–99] The DNP enhancement depends on γ_e/γ_n (the gyromagnetic ratios of the electron and polarised nucleus, respectively), meaning enhancement factors of up to ~658 can theoretically be obtained for ^{1}H. Although factors of 20–100 are more routinely observed in practice, this still reduces experimental times by factors of 400–10 000, enabling experiments that are unfeasible otherwise to become possible. In most cases, the unpaired electron originates from an external polarizing agent, typically a mono- or biradical species (such as TEMPO, TOTAPOL, bTbk, or AmuPOL), added by impregnating a powdered sample with the radical solution. As shown in Fig. 8(a), polarisation transfer to ^{1}H is achieved by high-power microwave irradiation of electron-nuclear transitions via one of a set of distinct mechanisms (e.g., the solid effect, cross effect, and Overhauser effect), depending on the system and conditions used. This polarisation is distributed throughout the sample via spin diffusion, before being transferred to heteronuclei (if desired) usually using CP. Direct DNP to heteronuclei is possible in principle, although this requires a sufficiently dense spin network to promote efficient spin diffusion and variation of the microwave frequency to match the relevant electron-nuclear transition. Low temperatures (~90 K) are routinely employed in DNP experiments to promote spin diffusion, increase the polarisation of the unpaired electrons, and lengthen proton relaxation times; DNP enhancement at 35 K has also been reported.[100] The enhancements achieved are governed by a number of factors, including microwave power, concentration and type of polarizing agent, temperature, solvent, and the relaxation times of the solute. Figures 8(c) and 8(d) show ^{13}C and ^{29}Si MAS NMR spectra of phenol-functionalized mesoporous silica impregnated with TOTAPOL in D_2O/H_2O 90:10 solution acquired with and without microwave irradiation, with enhancements of factors of ≥56 and ~21, respectively.

As DNP becomes more mainstream, there is an ongoing effort to extend its use to higher magnetic field strength. This would have a number of benefits, including increases in resolution and in the electron spin polarization. Challenges here, however, include incomplete excitation owing to the increasing width of the EPR lines, requiring an increase in microwave power.[99] Furthermore, some of the mechanisms of magnetisation transfer (e.g., the cross effect and solid effect) exploited in DNP decrease in efficiency at higher magnetic field, although recent work has shown that the Overhauser effect should increase as B_0 increases. Improvements in high-field DNP will therefore necessitate both a more detailed understanding of the mechanisms of DNP transfer and the development of novel polarizing agents with narrow EPR lines and long relaxation times.

The significant sensitivity advantages of DNP are clear, but its application is not without technical and practical challenges.[97,98] There is a significant cost implication for generating high-power microwaves, which is currently usually achieved using a gyrotron, although recent advances in the use of waveform generators offer considerable future potential in this area. As described above, the enhancements achieved depend crucially on many factors and are difficult to predict, giving DNP the appearance of a "black art" at times. The need for a dense ^{1}H network (or an equivalent network of high-γ spins) to promote the required spin diffusion and the inherent surface selectivity can restrict the application of DNP to particular systems, with the majority of studies to date on surfaces, nanoparticles, pharmaceuticals, and microporous

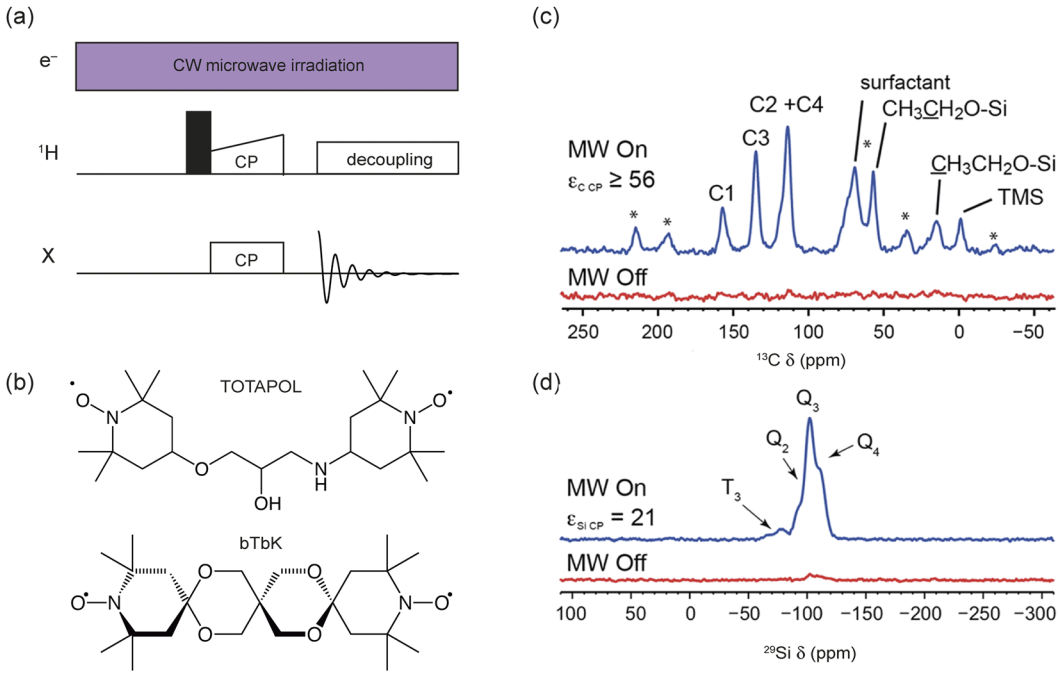

FIG. 8. (a) Pulse sequence for a DNP experiment using microwave irradiation to drive polarisation transfer to ^{1}H and CP for transfer to heteronuclei. (b) TOTAPOL and bTbK biradicals commonly used in DNP. (c) ^{13}C and (d) ^{29}Si CP MAS NMR spectra of phenol-functionalised silica impregnated with TOTAPOL in 90:10 D_2O/H_2O, acquired with (blue, higher) and without (red, lower) microwave irradiation. Adapted with permission from Rossini *et al.*, Acc. Chem. Res. **46**, 1942 (2013). Copyright 2013 American Chemical Society.

materials.[101] This surface selectivity, and the additional use of CP for heteronuclear experiments, also limits the quantitative information available. However, the potential advantages are so great that DNP may well herald a new dawn in the application of solid-state NMR spectroscopy and a true step change in the structural information available.

VI. CONCLUSIONS AND OUTLOOK

Continuing developments in methodology and hardware mean that solid-state NMR spectroscopy is now a mature and vital tool for structural characterisation of solids. Its sensitivity to the local structure means the information obtained is complementary to the average structural picture provided by other techniques. Researchers are increasingly aware that a detailed structural picture, combining information on different length scales, is critical to fully understanding structure-property relationships and ultimately directing materials design. Although previously somewhat in the shadow of its solution-state counterpart, it is now clear that solid-state NMR provides atomic-scale structural and mechanistic information that is simply not available using other approaches.

The main challenges associated with NMR spectroscopy in the solid state will remain the subject of ongoing research effort and technological development. The enduring quest for improved resolution has resulted in the development of hardware capable of rotating samples at ever faster MAS rates, the implementation of efficient and more effective decoupling sequences, and the increased availability of high magnetic field strengths. Although progress in this area will continue, it is likely that more sophisticated methods, perhaps many combining experiment and simulation in automated approaches, creating bespoke solutions for specific instruments, will be introduced in the near future. Sensitivity will always be a challenge for NMR, and for solid-state NMR, in particular. The use of composite pulses and the development of new pulse sequence methodology will continue to provide improvements in sensitivity for specific experiments, particularly for quadrupolar nuclei, but it seems increasingly likely that the major advances in this area will be provided by DNP. The improvements in signal-to-noise that have already been observed for many systems are sufficiently impressive that considerable effort will certainly be expended on optimising sample preparation and polarisation transfer, and widening the substrate scope of this approach. The current (considerable) hardware costs associated with DNP may also reduce as new approaches to microwave generation and the availability of increased microwave power are introduced. However, the current surface selectivity and non-quantitative nature of DNP mean that conventional solid-state NMR will continue to be the method of choice for many systems in the near future.

The development of polarisation transfer approaches and their application to a wider range of nuclear pairs and materials will undoubtedly continue, ensuring that a larger amount of increasingly more detailed structural information is available for complex systems. However, we believe that the most significant advance in understanding spectral signatures, and relating these to local structure, will come from the combined application of experiment and computation. Although a number of significant advances have been achieved in recent years, the potential for further improvement in this area is considerable. Continued development of improved DFT functionals, many body dispersion interactions, and accurate relativistic

corrections will increase the accuracy of the structural models used and the precision with which NMR parameters can be determined. Of particular interest would be the ability to routinely predict NMR parameters for paramagnetic systems, where the unusual (and temperature dependent) shifts observed hinder spectral assignment and structural interpretation. Although progress has been made for cluster calculations, its implementation into periodic codes would be a major advance. The interaction between theory and NMR experiment will also be very fruitful in the study of nuclear quantum effects (NQEs), i.e., going beyond the Born-Oppenheimer approximation and permitting delocalisation of the nuclear positions. Thanks to its sensitivity to local electronic structure, solid-state NMR parameters have already been shown to be highly sensitive to NQEs and powerful probes of the calculation methods under development.[102] As the accuracy and efficiency of computation increases, attention will undoubtedly turn to systems with increased chemical and/or topological complexity. While many have shown that insights into disordered systems can be obtained from sets of simpler calculations substituting small numbers of atoms, there are an increasing number of attempts to consider more realistic models for disordered materials, from systematically determining all possible atomic arrangements for systems exhibiting chemical disorder[103] to the use of other approaches, such as molecular mechanics or molecular dynamics,[65,77] to generate possible models for materials with positional or motional disorder. While technically possible at present, these approaches will expand and extend with ongoing hardware advances.

We hope we have demonstrated in this perspective how continued developments in hardware and methodology have pushed the resolving power of solid-state NMR to close to its limits. While sensitivity often limits the sophistication of experiments, the convergence of these advances with developments in quantum-chemical calculation have allowed the information encoded within the NMR spectra to be fully exploited. As a result, solid-state NMR can join its solution-state counterpart as a mainstream and essential tool for chemical characterisation.

[1] D. C. Apperley, R. K. Harris, and P. Hodgkinson, *Solid-State NMR: Basic Principles and Practice* (Momentum Press, New York, 2012).
[2] S. E. Ashbrook, D. M. Dawson, and J. M. Griffin, in *Local Structural Characterisation*, edited by D. W. Bruce, D. O'Hare, and R. I. Walton (Wiley-Blackwell, 2013), pp. 1–88.
[3] M. H. Levitt, *Spin Dynamics: Basics of Nuclear Magnetic Resonance*, 2nd ed. (John Wiley & Sons, 2008).
[4] V. E. Zorin, S. P. Brown, and P. Hodgkinson, J. Chem. Phys. **125**, 144508-1 (2006).
[5] P. K. Madhu, Solid State Nucl. Magn. Reson. **35**, 2 (2009).
[6] P. Hodgkinson, Ann. Rev. NMR Spectroc. **72**, 185 (2011).
[7] A. Ramamoorthy, *NMR Spectroscopy of Biological Solids* (CRC Press, 2005), p. 368.
[8] *Advances in Biological Solid-State NMR*, edited by F. Separovic and A. Naito (Royal Society of Chemistry, 2014).
[9] L. B. Andreas, T. Le Marchand, K. Jaudzems, and G. Pintacuda, J. Magn. Reson. **253**, 36 (2015).
[10] L. B. Andreas, K. Jaudzems, J. Stanek, D. Lalli, A. Bertarello, T. Le Marchand, D. Cala-De Paepe, S. Kotelovica, I. Akopjana, B. Knott, S. Wegner, F. Engelke, A. Lesage, L. Emsley, K. Tars, T. Herrmann, and G. Pintacuda, Proc. Natl. Acad. Sci. U. S. A. **113**, 9187 (2016).
[11] F. Fayon, I. J. King, R. K. Harris, R. K. B. Gover, J. S. O. Evans, and D. Massiot, Chem. Mater. **15**, 2234 (2003).
[12] A. Lesage, M. Bardet, and L. Emsley, J. Am. Chem. Soc. **121**, 10987 (1999).
[13] A. J. Robbins, W. T. K. Ng, D. Jochym, T. W. Keal, S. J. Clark, D. J. Tozer, and P. Hodgkinson, Phys. Chem. Chem. Phys. **9**, 2389 (2007).
[14] P. Hodgkinson, Prog. Nucl. Magn. Reson. Spectrosc. **46**, 197 (2005).
[15] V. E. Zorin, M. Ernst, S. P. Brown, and P. Hodgkinson, J. Magn. Reson. **192**, 183 (2008).
[16] P. K. Madhu, Isr. J. Chem. **54**, 25 (2014).
[17] I. Frantsuzov, M. Ernst, S. P. Brown, and P. Hodgkinson, Solid State Nucl. Magn. Reson. **70**, 28 (2015).
[18] I. Frantsuzov, S. K. Vasa, M. Ernst, S. P. Brown, V. Zorin, A. P. M. Kentgens, and P. Hodgkinson, ChemPhysChem **18**, 394 (2017).
[19] K. Xue, R. Sarkar, C. Motz, S. Asami, D. C. R. Camargo, V. Decker, S. Wegner, Z. Tosner, and B. Reif, Sci. Rep. **7**, 7444 (2017).
[20] S. E. Ashbrook and S. Sneddon, J. Am. Chem. Soc. **136**, 15440 (2014).
[21] A. Samoson, E. Lippmaa, and A. Pines, Mol. Phys. **65**, 1013 (1988).
[22] A. Llor and J. Virlet, Chem. Phys. Lett. **152**, 248 (1988).
[23] L. Frydman and J. S. Harwood, J. Am. Chem. Soc. **117**, 5367 (1995).
[24] A. Goldbourt and P. K. Madhu, in *Annual Reports on NMR Spectroscopy* (Academic Press, 2004), Vol. 54, pp. 81–153.
[25] Z. Gan, J. Am. Chem. Soc. **122**, 3242 (2000).
[26] S. E. Ashbrook and S. Wimperis, Prog. Nucl. Magn. Reson. Spectrosc. **45**, 53 (2004).
[27] S. E. Ashbrook, M. Cutajar, C. J. Pickard, R. I. Walton, and S. Wimperis, Phys. Chem. Chem. Phys. **10**, 5754 (2008).
[28] A. Kentgens, Prog. Nucl. Magn. Reson. Spectrosc. **32**, 141 (1998).
[29] L. Delevoye, J. Trébosc, Z. Gan, L. Montagne, and J.-P. Amoureux, J. Magn. Reson. **186**, 94 (2007).
[30] *NMR Crystallography*, edited by R. K. Harris, R. E. Wasylishen, and M. J. Duer (Wiley, 2012).
[31] D. L. Bryce and F. Taulelle, Acta Cryst. C **73**, 126 (2017) (editorial in special issue on NMR Crystallography; see all articles therein).
[32] L. Mafra, Solid State Nucl. Magn. Reson. **65**, 1 (2015) (preface of special issue on NMR Crystallography; see all articles therein).
[33] S. E. Ashbrook and D. McKay, Chem. Commun. **52**, 7186 (2016).
[34] See https://www.iucr.org/resources/commissions/nmr-crystallography for "Commission on NMR Crystallography and Related Methods" (last accessed April 04 2018).
[35] C. J. Pickard and F. Mauri, Phys. Rev. B **63**, 245101 (2001).
[36] C. Bonhomme, C. Gervais, F. Babonneau, C. Coelho, F. Pourpoint, T. Azais, S. E. Ashbrook, J. M. Griffin, J. R. Yates, and F. Mauri, Chem. Rev. **112**, 5733 (2012).
[37] W. Kohn and L. J. Sham, Phys. Rev. **140**, A1133 (1965).
[38] R. K. Harris, P. Hodgkinson, C. J. Pickard, V. Zorin, and J. R. Yates, Magn. Reson. Chem. **45**, S174 (2007).
[39] S. A. Joyce, J. R. Yates, C. J. Pickard, and F. Mauri, J. Chem. Phys. **127**, 204107 (2007).
[40] S. A. Joyce, J. R. Yates, C. J. Pickard, and S. P. Brown, J. Am. Chem. Soc. **130**, 12663 (2008).
[41] P. Sanz Camacho, K. S. Athukorala Arachchige, A. M. Slawin, T. F. Green, J. R. Yates, D. M. Dawson, J. D. Woollins, and S. E. Ashbrook, J. Am. Chem. Soc. **137**, 6172 (2015).
[42] P. Sanz Camacho, D. McKay, D. M. Dawson, C. Kirst, J. R. Yates, T. F. Green, D. B. Cordes, A. M. Slawin, J. D. Woollins, and S. E. Ashbrook, Inorg. Chem. **55**, 10881 (2016).
[43] J. D. Hartman, S. Monaco, B. Schatschneider, and G. J. O. Beran, J. Chem. Phys. **143**, 102809 (2015).
[44] J. R. Yates, S. E. Dobbins, C. J. Pickard, F. Mauri, P. Y. Ghi, and R. K. Harris, Phys. Chem. Chem. Phys. **7**, 1402 (2005).
[45] O. Socha, P. Hodgkinson, C. M. Widdifield, J. R. Yates, and M. Dračínský, J. Phys. Chem. A **121**, 4103 (2017).
[46] S. Grimme, J. Comput. Chem. **27**, 1787 (2006).
[47] D. V. Dudenko, J. R. Yates, K. D. Harris, and S. P. Brown, CrystEngComm **15**, 8797 (2013).
[48] S. Sneddon, D. M. Dawson, C. J. Pickard, and S. E. Ashbrook, Phys. Chem. Chem. Phys. **16**, 2660 (2014).
[49] M. Dračínský and P. Hodgkinson, CrystEngComm **15**, 8705 (2013).
[50] J. M. Stratford, M. Mayo, P. K. Allan, O. Pecher, O. J. Borkiewicz, K. M. Wiaderek, K. W. Chapman, C. J. Pickard, A. J. Morris, and C. P. Grey, J. Am. Chem. Soc. **139**, 7273 (2017).
[51] G. M. Day, Crystallogr. Rev. **17**, 3 (2011).
[52] C. J. Pickard and R. Needs, J. Phys.: Condens. Matter **23**, 053201 (2011).
[53] E. Salager, G. M. Day, R. S. Stein, C. J. Pickard, B. Elena, and L. Emsley, J. Am. Chem. Soc. **132**, 2564 (2010).

[54]K. A. See, M. Leskes, J. M. Griffin, S. Britto, P. D. Matthews, A. Emly, A. Van der Ven, D. S. Wright, A. J. Morris, and C. P. Grey, J. Am. Chem. Soc. **136**, 16368 (2014).
[55]R. F. Moran, D. McKay, C. J. Pickard, A. J. Berry, J. M. Griffin, and S. E. Ashbrook, Phys. Chem. Chem. Phys. **18**, 10173 (2016).
[56]M. Zilka, D. V. Dudenko, C. E. Hughes, P. A. Williams, S. Sturniolo, W. T. Franks, C. J. Pickard, J. R. Yates, K. D. Harris, and S. P. Brown, Phys. Chem. Chem. Phys. **19**, 25949 (2017).
[57]R. F. Moran, D. M. Dawson, and S. E. Ashbrook, Int. Rev. Phys. Chem. **36**, 39 (2017).
[58]P. Florian and F. Fayon, in *Modern Methods in Solid-State NMR: A Practitioner's Guide*, edited by P. Hodgkinson (The Royal Society of Chemistry, 2018), pp. 356–390.
[59]S. W. Reader, M. R. Mitchell, K. E. Johnston, C. J. Pickard, K. R. Whittle, and S. E. Ashbrook, J. Phys. Chem. C **113**, 18874 (2009).
[60]M. R. Mitchell, S. W. Reader, K. E. Johnston, C. J. Pickard, K. R. Whittle, and S. E. Ashbrook, Phys. Chem. Chem. Phys. **13**, 488 (2011).
[61]S. Cadars, N. Mifsud, A. Lesage, J. D. Epping, N. Hedin, B. F. Chmelka, and L. Emsley, J. Phys. Chem. C **112**, 9145 (2008).
[62]J. R. Peet, C. M. Widdifield, D. C. Apperley, P. Hodgkinson, M. R. Johnson, and I. R. Evans, Chem. Commun. **51**, 17163 (2015).
[63]M. Skotnicki, D. C. Apperley, J. A. Aguilar, B. Milanowski, M. Pyda, and P. Hodgkinson, Mol. Pharmaceutics **13**, 211 (2015).
[64]S. E. Lister, A. Soleilhavoup, R. L. Withers, P. Hodgkinson, and J. S. O. Evans, Inorg. Chem. **49**, 2290 (2010).
[65]T. Charpentier, M. C. Menziani, and A. Pedone, RSC Adv. **3**, 10550 (2013).
[66]J. Cuny, Y. Xie, C. J. Pickard, and A. A. Hassanali, J. Chem. Theory Comput. **12**, 765 (2016).
[67]D. M. Dawson and S. E. Ashbrook, J. Phys. Chem. C **118**, 23285 (2014).
[68]D. M. Dawson, V. R. Seymour, and S. E. Ashbrook, J. Phys. Chem. C **121**, 28065 (2017).
[69]P. Beckett, M. S. Denning, I. Heinmaa, M. C. Dimri, E. A. Young, R. Stern, and M. Carravetta, J. Chem. Phys. **137**, 114201 (2012).
[70]*Nuclear Magnetic Resonance Probes of Molecular Dynamics*, edited by R. Tycko (Springer Netherlands, 1994).
[71]D. Reichert and A. Krushelnitsky, in *Modern Methods in Solid-State NMR: A Practitioner's Guide*, edited by P. Hodgkinson (The Royal Society of Chemistry, 2018), pp. 161–192.
[72]R. Bohmer, M. Storek, and M. Vogel, in *Modern Methods in Solid-State NMR: A Practitioner's Guide*, edited by P. Hodgkinson (The Royal Society of Chemistry, 2018), pp. 193–230.
[73]P. Hodgkinson, in *Encyclopedia of Magnetic Resonance*, edited by R. K. Harris and R. E. Wasylishen (John Wiley, Chichester, 2009).
[74]H. E. Kerr, L. K. Softley, K. Suresh, A. Nangia, P. Hodgkinson, and I. R. Evans, CrystEngComm **17**, 6707 (2015).
[75]R. R. Vold, in *Nuclear Magnetic Resonance Probes of Molecular Dynamics*, edited by R. Tycko (Kluwer Academic Publishers, 1994), pp. 27–112.
[76]A. Abraham, D. C. Apperley, S. J. Byard, A. J. Ilott, A. J. Robbins, V. Zorin, R. K. Harris, and P. Hodgkinson, CrystEngComm **18**, 1054 (2016).
[77]A. J. Ilott, S. Palucha, A. S. Batsanov, M. R. Wilson, and P. Hodgkinson, J. Am. Chem. Soc. **132**, 5179 (2010).
[78]P. He, J. Xu, V. V. Terskikh, A. Sutrisno, H.-Y. Nie, and Y. Huang, J. Phys. Chem. C **117**, 16953 (2013).
[79]J. M. Griffin, L. Clark, V. R. Seymour, D. W. Aldous, D. M. Dawson, D. Iuga, R. E. Morris, and S. E. Ashbrook, Chem. Sci. **3**, 2293 (2012).
[80]G. P. Bignami, Z. H. Davis, D. M. Dawson, S. A. Morris, S. E. Russell, D. McKay, R. E. Parke, D. Iuga, R. E. Morris, and S. E. Ashbrook, Chem. Sci. **9**, 850 (2018).
[81]G. P. Bignami, D. M. Dawson, V. R. Seymour, P. S. Wheatley, R. E. Morris, and S. E. Ashbrook, J. Am. Chem. Soc. **139**, 5140 (2017).
[82]D. M. Dawson, L. E. Jamieson, M. I. H. Mohideen, A. C. McKinlay, I. A. Smellie, R. Cadou, N. S. Keddie, R. E. Morris, and S. E. Ashbrook, Phys. Chem. Chem. Phys. **15**, 919 (2013).
[83]C. Beumer, A. Konig, D. Scholzel, B. Uluca, F. Weirich, and H. Heise, in *Modern Methods in Solid-State NMR: A Practitioner's Guide*, edited by P. Hodgkinson (The Royal Society of Chemistry, 2018), pp. 289–321.
[84]T. Kobayashi, Y. Nishiyama, and M. Pruski, in *Modern Methods in Solid-State NMR: A Practitioner's Guide*, edited by P. Hodgkinson (The Royal Society of Chemistry, 2018), pp. 1–38.
[85]A. Pines, M. G. Gibby, and J. S. Waugh, J. Chem. Phys. **59**, 569 (1973).
[86]S. E. Ashbrook and S. Wimperis, Mol. Phys. **98**, 1 (2000).
[87]S. E. Ashbrook and S. Wimperis, J. Chem. Phys. **120**, 2719 (2004).
[88]S. E. Ashbrook and S. Wimperis, J. Chem. Phys. **131**, 194509 (2009).
[89]J.-P. Amoureux and M. Pruski, Mol. Phys. **100**, 1595 (2002).
[90]H. Y. Carr and E. M. Purcell, Phys. Rev. **94**, 630 (1954).
[91]S. Meiboom and D. Gill, Rev. Sci. Instrum. **29**, 688 (1958).
[92]T. T. Nakashima and R. E. Wasylishen, in *Encyclopedia of Magnetic Resonance*, edited by R. K. Harris and R. E. Wasylishen (John Wiley, Chichester, 2011).
[93]A. Kentgens and R. Verhagen, Chem. Phys. Lett. **300**, 435 (1999).
[94]P. Madhu, A. Goldbourt, L. Frydman, and S. Vega, Chem. Phys. Lett. **307**, 41 (1999).
[95]H. Colaux, D. M. Dawson, and S. E. Ashbrook, J. Phys. Chem. A **118**, 6018 (2014).
[96]H. Colaux, D. M. Dawson, and S. E. Ashbrook, Solid State Nucl. Magn. Reson. **84**, 89 (2017).
[97]A. J. Rossini, A. Zagdoun, M. Lelli, A. Lesage, C. Coperet, and L. Emsley, Acc. Chem. Res. **46**, 1942 (2013).
[98]Q. Z. Ni, E. Daviso, T. V. Can, E. Markhasin, S. K. Jawla, T. M. Swager, R. J. Temkin, J. Herzfeld, and R. G. Griffin, Acc. Chem. Res. **46**, 1933 (2013).
[99]A. S. L. Thankamony, J. J. Wittmann, M. Kaushik, and B. Corzilius, Prog. Nucl. Magn. Reson. Spectrosc. **102**, 120 (2017).
[100]E. Bouleau, P. Saint-Bonnet, F. Mentink-Vigier, H. Takahashi, J. F. Jacquot, M. Bardet, F. Aussenac, A. Purea, F. Engelke, S. Hediger, D. Lee, and G. De Paëpe, Chem. Sci. **6**, 6806 (2015).
[101]R. Griffin and T. Prisner, Phys. Chem. Chem. Phys. **12**, 5737 (2010).
[102]M. Dračínský and P. Hodgkinson, Chem.–Eur. J. **20**, 2201 (2014).
[103]R. Grau-Crespo, S. Hamad, C. R. A. Catlow, and N. De Leeuw, J. Phys.: Condens. Matter **19**, 256201 (2007).